

Cooperative two-photon absorption. II

David L. Andrews and Michael J. Harlow

School of Chemical Sciences, University of East Anglia, Norwich NR4 7TJ, England

(Received 23 November 1983; accepted 6 February 1984)

In this paper we extend our earlier work on cooperative two-photon absorption to the case of one- and three-photon allowed transitions using the principles of quantum electrodynamics. After deriving a general rate equation we consider two specific molecular systems: (i) van der Waals molecules in which the two centers have a fixed mutual orientation; and (ii) fluid samples with random molecular orientation. Calculations are shown to involve a new type of rotational average which gives rise to two-photon circular dichroism in case (i). The dependence of the rate upon molecular separation is discussed in detail, as is the possibility of resonance enhancement if suitable intermediate energy levels are present. Finally we draw attention to an effect specific to this mode of cooperative absorption and speculate on the possibility of direct observation of the effects of retardation.

I. INTRODUCTION

In a recent paper¹ (hereafter referred to as paper I) we discussed in some detail the process of cooperative two-photon absorption, in which a pair of molecules or chromophores undergo the concerted absorption of two photons, with the result that both become excited. In the formalism of quantum electrodynamics the interaction between the molecules is mediated by a virtual photon, and there are two mechanisms leading to excitation, which are differentiated by the selection rules of the individual molecules.

In the first case, considered in paper I, the two molecular transitions are separately allowed under two-photon selection rules, and each molecule absorbs one laser photon and either emits or absorbs the virtual photon. In the second case, which we discuss in this paper, two-photon transitions are forbidden and the excitation occurs through one- and three-photon transitions. In this case both the laser photons are absorbed by one of the molecules and the second is excited via the virtual photon coupling. For convenience we shall refer to the former as the 2,2-allowed mode or mechanism, and the latter as the 1,3-allowed mode.

The theoretical approach is the same in both cases, but it is shown that the dissymmetry of the 1,3-allowed mode leads to a more complicated initial rate equation, and that when the rate for van der Waals molecules is considered a new type of rotational average is required. One result of this is the manifestation of two-photon circular dichroism in the case of molecules with a fixed mutual orientation. Further conventional rotational averages subsequently yield the rate equation for a fluid system in which the molecular orientation is entirely random.

The fully quantum electrodynamical treatment leads to results which are generally valid for any intermolecular separation, and which naturally incorporate retardation effects which significantly modify the results at large separations. In the Discussion section we give full details of the effects of retardation on the form of the rate equations, and we also consider the possibility of resonance enhancement of the process in molecules with suitable energy levels. After considering the absolute magnitude of the cooperative two-

photon absorption rate we conclude by noting an effect peculiar to the 1,3-allowed mode, and postulate a directly observable manifestation of retardation.

II. THEORY

The results presented in this paper are derived from quantum electrodynamical calculations in which energy is transferred between a pair of molecules by virtual photon coupling; full details of this approach may be found in paper I.¹ As before, the process of interest is that in which the molecules labeled A and B are cooperatively excited via virtual intermediate states to final states $|\alpha\rangle$ and $|\beta\rangle$, respectively, through the absorption of two laser photons. The incident light is characterized by frequency ω , wave vector \mathbf{k} , and polarization \mathbf{e} , and the cooperative absorption process satisfies the energy conservation relation

$$2\hbar\omega = E_{\alpha 0} + E_{\beta 0}. \quad (2.1)$$

Once again, we represent the state vector of the system at any stage of the interaction by $|a;b;n_r;n_v\rangle$, where $|a\rangle$ is the state vector of molecule A, $|b\rangle$ refers to molecule B, and n_r and n_v denote the numbers of real (laser) photons and virtual photons, respectively. Hence the initial and final states of the system are

$$|i\rangle = |0;0;n;0\rangle \quad (2.2)$$

and

$$|f\rangle = |\alpha;\beta;n-2;0\rangle. \quad (2.3)$$

In contrast to our previous treatment, we now consider the case in which the transitions $|\alpha\rangle \leftarrow |0\rangle$ and $|\beta\rangle \leftarrow |0\rangle$ are one-photon allowed, but two-photon forbidden in the isolated molecules. In this case the leading contributions to the matrix element for the process, which result from fourth-order time-dependent perturbation theory, are illustrated by time-ordered diagrams such as those shown in Fig. 1. Each of the four diagrams (a)–(d) is representative of a set of six which differ only in the time ordering of the molecule-photon interactions.

It should be noted that, whereas in the 12 diagrams represented by Figs. 1(a) and 1(b), the transition $|\alpha\rangle \leftarrow |0\rangle$ is

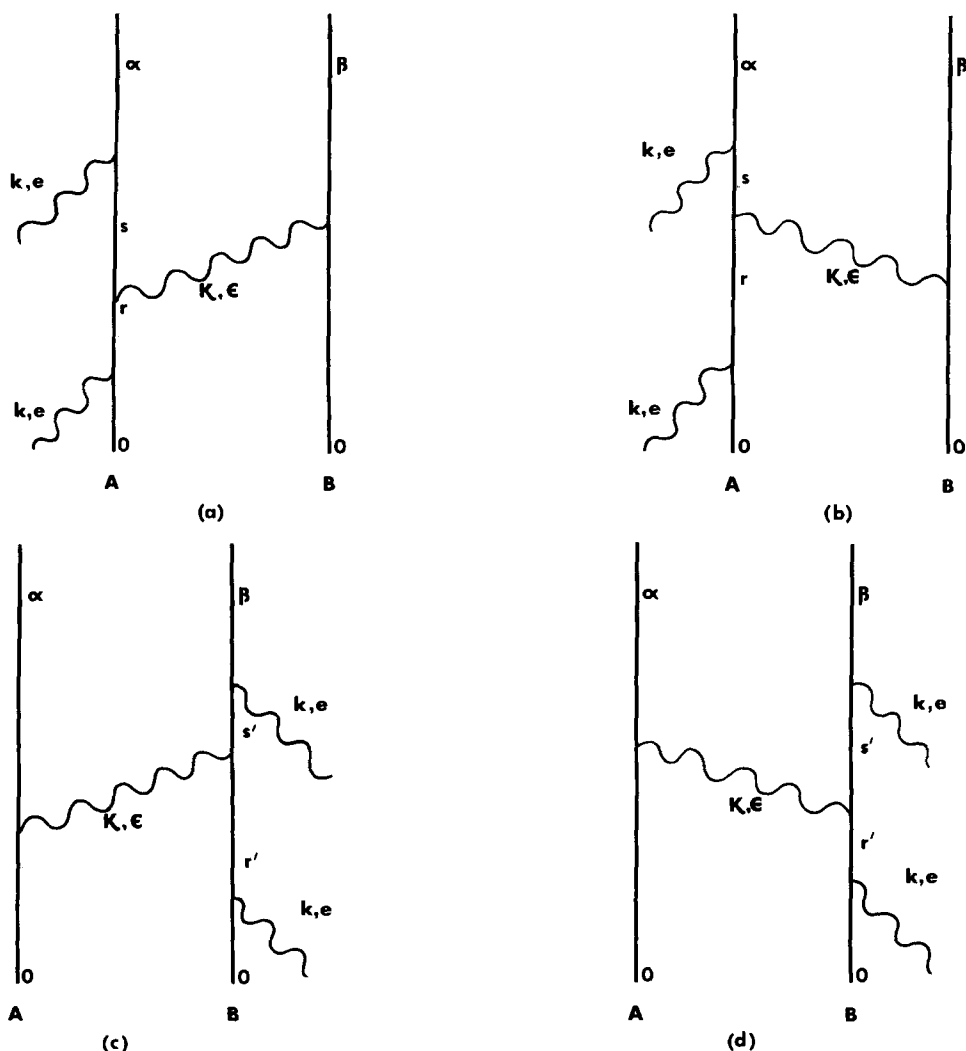


FIG. 1. Typical time-ordered diagrams for cooperative two-photon absorption.

allowed by three-photon selection rules and $|\beta\rangle \leftarrow |0\rangle$ is one photon allowed, the converse is true for the 12 diagrams represented by Figs. 1(c) and 1(d). Hence in a specific application it is possible that one or other of the transitions may be one-photon forbidden, but three-photon allowed, so that 12 of the diagrams become redundant, and the corresponding contribution to the matrix element disappears. Clearly, however, it is necessary for at least one of the transitions at A or B to be allowed under one-photon selection rules for this type of cooperative mechanism to apply. We also note that any transition allowed under single-photon selection rules is also three-photon allowed.

In general the 24 separate contributions to the matrix element may be written down by reference to the time-ordered diagrams in the usual way; the contribution corresponding to Fig. 1(a), for example, is as follows;

$$\begin{aligned} & \sum_r \sum_s \sum_k \sum_\epsilon \langle \alpha; \beta; n-2; 0 | -\boldsymbol{\mu} \cdot \mathbf{d}^\dagger | s; \beta; n-1; 0 \rangle \\ & \times \langle s; \beta; n-1; 0 | -\boldsymbol{\mu} \cdot \mathbf{d}^\dagger | s; 0; n-1; 1 \rangle \\ & \times \langle s; 0; n-1; 1 | -\boldsymbol{\mu} \cdot \mathbf{d}^\dagger | r; 0; n-1; 0 \rangle \\ & \times \langle r; 0; n-1; 0 | -\boldsymbol{\mu} \cdot \mathbf{d}^\dagger | 0; 0; n; 0 \rangle \\ & \times \{ (E_{0s} + E_{0\beta} + \hbar\omega)(E_{0s} + \hbar\omega - \hbar\omega)(E_{0r} + \hbar\omega) \}^{-1}, \end{aligned} \quad (2.4)$$

where the transverse electric displacement operator is given by

$$\mathbf{d}^\dagger(\mathbf{r}) = \sum_{\mathbf{k}, \lambda} \left(\frac{2\pi\hbar c k}{V} \right)^{1/2} i [e^{i\lambda}(\mathbf{k}) a^{(\lambda)}(\mathbf{k}) e^{i\mathbf{k} \cdot \mathbf{r}} - \bar{e}^{i\lambda}(\mathbf{k}) a^{\dagger(\lambda)}(\mathbf{k}) e^{-i\mathbf{k} \cdot \mathbf{r}}],$$

and $\boldsymbol{\mu}$ is the electric dipole operator: the inner summation in Eq.(2.4) is taken over the wave vector $\boldsymbol{\kappa}$ and polarization ϵ of the virtual photon. By summing all such contributions, the complete matrix element may be expressed as follows, as the sum of four tensors representing each class of time-ordered diagram;

$$\begin{aligned} M_{fi} = & - \left(\frac{2\pi\hbar}{V} \right)^2 c\omega n^{1/2} (n-1)^{1/2} e_i e_j \\ & \times \sum_{\mathbf{k}, \epsilon} \boldsymbol{\kappa} \epsilon_k \bar{\epsilon}_l \left[\left\{ \frac{\chi_{ijl}^{\alpha 0} \mu_k^{\beta 0}}{E_{\beta 0} - \hbar\omega} \right\} e^{i\mathbf{k} \cdot \mathbf{R}} \right. \\ & + \left\{ \frac{\chi_{ijk}^{\alpha 0} \mu_l^{\beta 0}}{E_{\beta 0} - \hbar\omega} \right\} e^{-i\mathbf{k} \cdot \mathbf{R}} \\ & + \left\{ \frac{\chi_{ijk}^{\beta 0} \mu_l^{\alpha 0}}{E_{\alpha 0} - \hbar\omega} \right\} e^{i(2\mathbf{k} + \boldsymbol{\kappa}) \cdot \mathbf{R}} \\ & \left. + \left\{ \frac{\chi_{ijl}^{\beta 0} \mu_k^{\alpha 0}}{E_{\alpha 0} - \hbar\omega} \right\} e^{i(2\mathbf{k} - \boldsymbol{\kappa}) \cdot \mathbf{R}} \right]. \end{aligned} \quad (2.5)$$

Here the factor $n^{1/2}(n-1)^{1/2}$ arises through successive application of the annihilation term in the electric displacement operator for the two real photon absorption events; μ^{f_0} represents the electric dipole transition moment for the transition $|f\rangle \leftarrow |0\rangle$, and the tensor $\chi_{ijk}^{f_0}$ is given by the expression

$$\chi_{ijk}^{f_0} = \frac{1}{2} \sum_{r,s} \left[\frac{\mu_i^{r_0} \mu_j^{sr} \mu_k^{fs}}{(E_{0s} + 2\hbar\omega)(E_{0r} + \hbar\omega)} + \frac{\mu_i^{r_0} \mu_j^{fs} \mu_k^{sr}}{(E_{fs} - \hbar\omega)(E_{0r} + \hbar\omega)} + \frac{\mu_i^{sr} \mu_j^{fs} \mu_k^{r_0}}{(E_{fs} - \hbar\omega)(E_{fr} - 2\hbar\omega)} + \frac{\mu_i^{sr} \mu_j^{r_0} \mu_k^{fs}}{(E_{0s} + 2\hbar\omega)(E_{0r} + \hbar\omega)} + \frac{\mu_i^{fs} \mu_j^{r_0} \mu_k^{sr}}{(E_{fs} - \hbar\omega)(E_{0r} + \hbar\omega)} + \frac{\mu_i^{fs} \mu_j^{sr} \mu_k^{r_0}}{(E_{fs} - \hbar\omega)(E_{fr} - 2\hbar\omega)} \right]. \quad (2.6)$$

This tensor is exactly identical to the hyper-Raman transition tensor $\beta_{kij}^{f_0,2}$.

After performing the virtual photon wave vector and polarization summation³ in Eq. (2.5), the result may be expressed as

$$M_{fi} = \frac{-8\pi^2 \hbar\omega}{V} n^{1/2}(n-1)^{1/2} e_i e_j \times [\chi_{ijk}^{\alpha_0} \mu_i^{\beta_0} V_{kl}(p, \mathbf{R}) + \chi_{ijk}^{\beta_0} \mu_i^{\alpha_0} V_{kl}(q, \mathbf{R}) e^{2ik \cdot \mathbf{R}}]. \quad (2.7)$$

Here p and q are defined by the relations

$$\hbar cp = E_{\beta_0}, \quad (2.8)$$

$$\hbar cq = E_{\alpha_0}, \quad (2.9)$$

and represent the energy transferred between the molecules during the cooperative absorption process. The retarded electric-dipole electric-dipole interaction tensor $V_{kl}(\gamma, \mathbf{R})$ is given by

$$V_{kl}(\gamma, \mathbf{R}) = \frac{1}{4\pi R^3} [F(\gamma, R) \delta_{kl} + G(\gamma, R) \hat{R}_k \hat{R}_l], \quad (2.10)$$

where

$$F(\gamma, R) = \cos \gamma R + \gamma R \sin \gamma R - \gamma^2 R^2 \cos \gamma R, \quad (2.11)$$

$$G(\gamma, R) = -3 \cos \gamma R - 3\gamma R \sin \gamma R + \gamma^2 R^2 \cos \gamma R. \quad (2.12)$$

Using the Fermi rule,⁴ the rate of cooperative two-photon absorption may be calculated from Eq. (2.7), giving the following result;

$$\Gamma = K e_i e_j \bar{e}_m \bar{e}_n [\chi_{ijk}^{\alpha_0} \mu_i^{\beta_0} \bar{\chi}_{mno}^{\alpha_0} \bar{\mu}_p^{\beta_0} V_{kl}(p, \mathbf{R}) V_{op}(p, \mathbf{R}) + \chi_{ijk}^{\beta_0} \mu_i^{\alpha_0} \bar{\chi}_{mno}^{\beta_0} \bar{\mu}_p^{\alpha_0} V_{kl}(q, \mathbf{R}) V_{op}(q, \mathbf{R}) + \chi_{ijk}^{\beta_0} \mu_i^{\alpha_0} \bar{\chi}_{mno}^{\alpha_0} \bar{\mu}_p^{\beta_0} V_{kl}(q, \mathbf{R}) V_{op}(p, \mathbf{R}) e^{2ik \cdot \mathbf{R}} + \chi_{ijk}^{\alpha_0} \mu_i^{\beta_0} \bar{\chi}_{mno}^{\beta_0} \bar{\mu}_p^{\alpha_0} V_{kl}(p, \mathbf{R}) V_{op}(q, \mathbf{R}) e^{-2ik \cdot \mathbf{R}}], \quad (2.13)$$

where

$$K = \frac{128\pi^5 I^2 g^{(2)} \rho_F}{\hbar c^2}. \quad (2.14)$$

Here ρ_F is the density of final states, I is the mean irradiance of the laser beam, and $g^{(2)}$ its degree of second order coherence.

A notable feature of Eq. (2.13) is the appearance of cross terms resulting from the interference of probability amplitudes for two-photon absorption at A and B. No such cross terms arose in the case considered previously,¹ in which both molecules absorbed a single laser photon; this difference has important implications for the response to circularly polarized light as will be demonstrated below. The result is directly applicable to the situation where each pair of molecules which may undergo a cooperative transition is held in a fixed orientation relative to the laser radiation, as for example in a molecular crystal. In order to apply the result to fluid samples, however, orientational averaging of the equation is required; there are two distinct cases to consider, which are dealt with in the following sections.

III. TWO MOLECULES IN A FIXED MUTUAL ORIENTATION

First we consider the case where the relative orientation of molecules A and B is fixed, but the A-B system is free to rotate in the laser beam. The results derived are thus applicable to certain van der Waals molecules, or to other large molecules in which A and B represent independent chromophores. In order to derive results which are appropriate for such species, it is necessary to perform a single rotational average of Eq. (2.13). To accomplish this, we first specify a laboratory-fixed Cartesian reference frame denoted by p in which the laser polarization vectors are fixed, and a frame for the A-B system (which for convenience may be defined to have its origin at center A) denoted by a , in which the molecular tensors and the vector \mathbf{R} are fixed. Hence Eq. (2.13) may be expressed as

$$\Gamma = K e_{p_i} e_{p_j} \bar{e}_{p_m} \bar{e}_{p_n} l_{p_i a_i} l_{p_j a_j} l_{p_m a_m} l_{p_n a_n} \times [\chi_{a_i a_j a_k}^{\alpha_0} \mu_{a_i}^{\beta_0} \bar{\chi}_{a_m a_n a_o}^{\alpha_0} \bar{\mu}_{a_p}^{\beta_0} V_{a_k a_l}(p, \mathbf{R}) V_{a_o a_p}(p, \mathbf{R}) + \chi_{a_i a_j a_k}^{\beta_0} \mu_{a_i}^{\alpha_0} \bar{\chi}_{a_m a_n a_o}^{\beta_0} \bar{\mu}_{a_p}^{\alpha_0} V_{a_k a_l}(q, \mathbf{R}) V_{a_o a_p}(q, \mathbf{R}) + \chi_{a_i a_j a_k}^{\beta_0} \mu_{a_i}^{\alpha_0} \bar{\chi}_{a_m a_n a_o}^{\alpha_0} \bar{\mu}_{a_p}^{\beta_0} V_{a_k a_l}(q, \mathbf{R}) V_{a_o a_p}(p, \mathbf{R}) e^{2ik \cdot \mathbf{R}} + \chi_{a_i a_j a_k}^{\alpha_0} \mu_{a_i}^{\beta_0} \bar{\chi}_{a_m a_n a_o}^{\beta_0} \bar{\mu}_{a_p}^{\alpha_0} V_{a_k a_l}(p, \mathbf{R}) V_{a_o a_p}(q, \mathbf{R}) e^{-2ik \cdot \mathbf{R}}] \quad (3.1)$$

in which $l_{p_i a_i}$ is the direction cosine between the p_i and a_i directions.

In the first two terms of Eq. (3.1) the vectors and tensors are referred to Cartesian frames in which they are rotationally invariant, and hence rotational averaging may be effected by averaging the direction cosine product alone. However, in the third and fourth terms of this equation, the exponentials also include orientation-dependent phase factors involving the scalar product $\mathbf{k} \cdot \mathbf{R}$, which must also be included in the averaging. We thus require the following result:

$$\begin{aligned} \Gamma = & K e_{p_i} e_{p_j} \bar{e}_{p_m} \bar{e}_{p_n} [\chi_{a_i a_j}^{\alpha 0} \bar{\chi}_{j i o}^{\alpha 0} \mu_{a_i}^{\beta 0} \bar{\mu}_{j o}^{\beta 0} V_{a_i a_j}(p, \mathbf{R}) V_{a_i a_j}(p, \mathbf{R}) \langle l_{p_i} l_{p_j} l_{p_m} l_{p_n} \rangle \\ & + \chi_{a_i a_j}^{\beta 0} \bar{\chi}_{j i o}^{\alpha 0} \mu_{a_i}^{\alpha 0} \bar{\mu}_{j o}^{\beta 0} V_{a_i a_j}(q, \mathbf{R}) V_{a_i a_j}(q, \mathbf{R}) \langle l_{p_i} l_{p_j} l_{p_m} l_{p_n} \rangle \\ & + \chi_{a_i a_j}^{\beta 0} \bar{\chi}_{j i o}^{\alpha 0} \mu_{a_i}^{\alpha 0} \bar{\mu}_{j o}^{\beta 0} V_{a_i a_j}(q, \mathbf{R}) V_{a_i a_j}(p, \mathbf{R}) \langle l_{p_i} l_{p_j} l_{p_m} l_{p_n} \rangle e^{2i\mathbf{k} \cdot \mathbf{R}} \\ & + \chi_{a_i a_j}^{\alpha 0} \bar{\chi}_{j i o}^{\beta 0} \mu_{a_i}^{\beta 0} \bar{\mu}_{j o}^{\alpha 0} V_{a_i a_j}(p, \mathbf{R}) V_{a_i a_j}(q, \mathbf{R}) \langle l_{p_i} l_{p_j} l_{p_m} l_{p_n} \rangle e^{-2i\mathbf{k} \cdot \mathbf{R}}]. \end{aligned} \quad (3.2)$$

The average of the direction cosine product in the first two terms of Eq. (3.2) is easily calculated by standard methods and is a well-known result.⁵ However, averages of the type appearing in the third and fourth terms require a different treatment, and the results have only recently been evaluated.⁶ Inserting the results for these averages into Eq. (3.2) leads to the following result:

$$\begin{aligned} \Gamma = & \frac{K}{840} [56 \{ \chi_{i i k}^{\alpha 0} \bar{\chi}_{j j o}^{\alpha 0} (2\eta - 1) + \chi_{i j k}^{\alpha 0} \bar{\chi}_{j i o}^{\alpha 0} (3 - \eta) \} \mu_i^{\beta 0} \bar{\mu}_p^{\beta 0} V_{kl}(p, \mathbf{R}) V_{op}(p, \mathbf{R}) \\ & + 56 j_0(2kR) \{ \chi_{i i k}^{\beta 0} \bar{\chi}_{j j o}^{\alpha 0} (2\eta - 1) + \chi_{i j k}^{\beta 0} \bar{\chi}_{j i o}^{\alpha 0} (3 - \eta) \} \mu_i^{\alpha 0} \bar{\mu}_p^{\beta 0} V_{kl}(q, \mathbf{R}) V_{op}(p, \mathbf{R}) \\ & + 336 i j_1(2kR) (\zeta) \epsilon_{i m l} \hat{R}_i \chi_{i j k}^{\beta 0} \bar{\chi}_{j m o}^{\alpha 0} \mu_i^{\alpha 0} \bar{\mu}_p^{\beta 0} V_{kl}(q, \mathbf{R}) V_{op}(p, \mathbf{R}) \\ & - 20 j_2(2kR) \{ 2 \chi_{i i k}^{\beta 0} \bar{\chi}_{m m o}^{\alpha 0} (5\eta - 4) + 4 \chi_{i j k}^{\beta 0} \bar{\chi}_{j i o}^{\alpha 0} (3 - 2\eta) \\ & - 3 \chi_{i j k}^{\beta 0} \bar{\chi}_{m m o}^{\alpha 0} \hat{R}_i \hat{R}_j (5\eta - 4) - 3 \chi_{i i k}^{\beta 0} \bar{\chi}_{m n o}^{\alpha 0} \hat{R}_m \hat{R}_n (5\eta - 4) \\ & - 12 \chi_{i j k}^{\beta 0} \bar{\chi}_{j m o}^{\alpha 0} \hat{R}_i \hat{R}_m (3 - 2\eta) \} \mu_i^{\alpha 0} \bar{\mu}_p^{\beta 0} V_{kl}(q, \mathbf{R}) V_{op}(p, \mathbf{R}) \\ & + 84 i j_3(2kR) (\zeta) \epsilon_{i m l} \hat{R}_i \{ 5 \chi_{i j k}^{\beta 0} \bar{\chi}_{m n o}^{\alpha 0} \hat{R}_j \hat{R}_n - \chi_{i j k}^{\beta 0} \bar{\chi}_{j m o}^{\alpha 0} \} \mu_i^{\alpha 0} \bar{\mu}_p^{\beta 0} V_{kl}(q, \mathbf{R}) V_{op}(p, \mathbf{R}) \\ & + 3 j_4(2kR) (2 + \eta) \{ 35 \chi_{i j k}^{\beta 0} \bar{\chi}_{m n o}^{\alpha 0} \hat{R}_i \hat{R}_j \hat{R}_m \hat{R}_n - 5 \chi_{i i k}^{\beta 0} \bar{\chi}_{m n o}^{\alpha 0} \hat{R}_m \hat{R}_n - 5 \chi_{i j k}^{\beta 0} \bar{\chi}_{j i o}^{\alpha 0} \hat{R}_i \hat{R}_j - 20 \chi_{i j k}^{\beta 0} \bar{\chi}_{i n o}^{\alpha 0} \hat{R}_j \hat{R}_n \\ & + \chi_{i i k}^{\beta 0} \bar{\chi}_{j j o}^{\alpha 0} + 2 \chi_{i j k}^{\beta 0} \bar{\chi}_{j i o}^{\alpha 0} \} \mu_i^{\alpha 0} \bar{\mu}_p^{\beta 0} V_{kl}(q, \mathbf{R}) V_{op}(p, \mathbf{R}) \\ & + \text{terms obtained from the transposition } (\alpha, p \leftrightarrow \beta, q)]. \end{aligned} \quad (3.3)$$

In Eq. (3.3), j_n are the spherical Bessel functions of the first kind, and η and ζ are polarization parameters defined by

$$\eta = (\mathbf{e} \cdot \mathbf{e})(\bar{\mathbf{e}} \cdot \bar{\mathbf{e}}), \quad (3.4)$$

$$\zeta = (\mathbf{e} \times \bar{\mathbf{e}}) \cdot \hat{\mathbf{k}}. \quad (3.5)$$

We note that η assumes the value of unity for plane polarized light and zero for circularly polarized light; by contrast ζ is zero for plane polarized light but for circularly polarized light we have

$$\zeta^{(L)} = -i \text{ and } \zeta^{(R)} = i. \quad (3.6)$$

Hence the j_1 and j_3 terms in Eq. (3.3) only contribute to the result in the case of circularly polarized radiation, and their sign depends on the handedness of the incident light. Consequently, two-photon circular dichroism is exhibited in the cooperative absorption process for molecules with a fixed mutual orientation.

The extent of circular dichroism may be expressed through the ratio of the difference in rates for left- and right-circular polarization and the mean rate, i.e.,

$$\Delta^{(L/R)} = \frac{\Gamma^{(L)} - \Gamma^{(R)}}{\frac{1}{2}(\Gamma^{(L)} + \Gamma^{(R)})} \quad (3.7)$$

which, using Eqs. (3.3) and (3.6), gives

$$\Delta^{(L/R)} = \frac{c j_1(2kR) + e j_3(2kR)}{a + b j_0(2kR) + d j_2(2kR) + f j_4(2kR)}, \quad (3.8)$$

where

$$a = 56(3 \chi_{i j k}^{\alpha 0} \bar{\chi}_{j i o}^{\alpha 0} - \chi_{i i k}^{\alpha 0} \bar{\chi}_{j j o}^{\alpha 0}) \mu_i^{\beta 0} \bar{\mu}_p^{\beta 0} V_{kl}(p, \mathbf{R}) V_{op}(p, \mathbf{R}) + (\alpha, p \leftrightarrow \beta, q), \quad (3.9)$$

$$b = 56(3 \chi_{i j k}^{\beta 0} \bar{\chi}_{j i o}^{\alpha 0} - \chi_{i i k}^{\beta 0} \bar{\chi}_{j j o}^{\alpha 0}) \mu_i^{\alpha 0} \bar{\mu}_p^{\beta 0} V_{kl}(p, \mathbf{R}) V_{op}(p, \mathbf{R}) + (\alpha, p \leftrightarrow \beta, q), \quad (3.10)$$

$$c = 672 \epsilon_{i m l} \hat{R}_i \chi_{i j k}^{\beta 0} \bar{\chi}_{j m o}^{\alpha 0} \mu_i^{\alpha 0} \bar{\mu}_p^{\beta 0} V_{kl}(q, \mathbf{R}) V_{op}(p, \mathbf{R}) + (\alpha, p \leftrightarrow \beta, q), \quad (3.11)$$

$$\begin{aligned} d = & 20(8 \chi_{i i k}^{\beta 0} \bar{\chi}_{j j o}^{\alpha 0} - 12 \chi_{i j k}^{\beta 0} \bar{\chi}_{j i o}^{\alpha 0} - 12 \chi_{i j k}^{\beta 0} \bar{\chi}_{j m o}^{\alpha 0} \hat{R}_i \hat{R}_j - 12 \chi_{i i k}^{\beta 0} \bar{\chi}_{m n o}^{\alpha 0} \hat{R}_m \hat{R}_n + 36 \chi_{i j k}^{\beta 0} \bar{\chi}_{j m o}^{\alpha 0} \hat{R}_i \hat{R}_m) \\ & \times \mu_i^{\alpha 0} \bar{\mu}_p^{\beta 0} V_{kl}(q, \mathbf{R}) V_{op}(p, \mathbf{R}) + (\alpha, p \leftrightarrow \beta, q), \end{aligned} \quad (3.12)$$

$$e = 168 \epsilon_{i m l} \hat{R}_i (5 \chi_{i j k}^{\beta 0} \bar{\chi}_{m n o}^{\alpha 0} \hat{R}_j \hat{R}_n - \chi_{i j k}^{\beta 0} \bar{\chi}_{j m o}^{\alpha 0}) \mu_i^{\alpha 0} \bar{\mu}_p^{\beta 0} V_{kl}(q, \mathbf{R}) V_{op}(p, \mathbf{R}) + (\alpha, p \leftrightarrow \beta, q), \quad (3.13)$$

$$\begin{aligned} f = & 6(35 \chi_{i j k}^{\beta 0} \bar{\chi}_{m n o}^{\alpha 0} \hat{R}_i \hat{R}_j \hat{R}_m \hat{R}_n - 5 \chi_{i i k}^{\beta 0} \bar{\chi}_{m n o}^{\alpha 0} \hat{R}_m \hat{R}_n - 5 \chi_{i j k}^{\beta 0} \bar{\chi}_{j i o}^{\alpha 0} \hat{R}_i \hat{R}_j - 20 \chi_{i j k}^{\beta 0} \bar{\chi}_{i n o}^{\alpha 0} \hat{R}_j \hat{R}_n \\ & + \chi_{i i k}^{\beta 0} \bar{\chi}_{j j o}^{\alpha 0} + 2 \chi_{i j k}^{\beta 0} \bar{\chi}_{j i o}^{\alpha 0}) \mu_i^{\alpha 0} \bar{\mu}_p^{\beta 0} V_{kl}(q, \mathbf{R}) V_{op}(p, \mathbf{R}) + (\alpha, p \leftrightarrow \beta, q). \end{aligned} \quad (3.14)$$

Both the results (3.3) and (3.8) are applicable to a system with any separation of the centers A and B. However, in the context of this section we are specifically considering a system in which the intermolecular distance R is fixed, and is generally within the near zone defined by $(2kR, pR, qR) \ll 1$ or $(2k, p, q) \ll R^{-1}$. The R dependence of the rate equation (3.3) arises from the Bessel functions $j_n(2kR)$ and the retarded electric-dipole tensors $V(q, \mathbf{R})$ and $V(p, \mathbf{R})$; so by considering the

limiting forms of these functions as $R \rightarrow 0$, the near-zone behavior of the rate may be found. The retarded electric-dipole electric-dipole tensor is given in Eq. (2.10), and in the near zone we have,

$$\lim_{pR \ll 1} F(p, R) = 1; \quad (3.15)$$

$$\lim_{pR \ll 1} G(p, R) = -3. \quad (3.16)$$

The only Bessel function which gives a significant contribution in the near zone is $j_0(2kR)$ such that

$$\lim_{2kR \ll 1} j_0(2kR) = 1. \quad (3.17)$$

The near-zone behavior follows directly on application of Eqs. (3.15)–(3.17) to Eq. (3.3) and essentially involves only the first two terms in that equation, leading to an R^{-6} dependence of the rate.

The differential rate may be treated in a similar way by taking the dominant terms in the numerator and denominator of Eq. (3.8), with the result that

$$\Delta^{(L/R)} = \left(\frac{x}{y} \right) kR, \quad (3.18)$$

where

$$x = 448\epsilon_{iml}\hat{R}_l \left[\left\{ \chi_{ijk}^{\beta 0 \bar{\alpha} 0} \bar{\mu}_k^{\alpha 0 \bar{\beta} 0} - 3\chi_{ijk}^{\beta 0 \bar{\alpha} 0} \bar{\mu}_k^{\alpha 0 \bar{\beta} 0} \hat{R}_o \hat{R}_p - 3\chi_{ijk}^{\beta 0 \bar{\alpha} 0} \bar{\mu}_l^{\alpha 0 \bar{\beta} 0} \hat{R}_k \hat{R}_l \right. \right. \\ \left. \left. + 9\chi_{ijk}^{\beta 0 \bar{\alpha} 0} \bar{\mu}_l^{\alpha 0 \bar{\beta} 0} \hat{R}_k \hat{R}_l \hat{R}_o \hat{R}_p \right\} + \{\alpha \leftrightarrow \beta\} \right], \quad (3.19)$$

$$y = 56 \left[-\chi_{iik}^{\alpha 0 \bar{\alpha} 0} \bar{\mu}_k^{\beta 0 \bar{\beta} 0} + 3\chi_{iik}^{\alpha 0 \bar{\alpha} 0} \bar{\mu}_k^{\beta 0 \bar{\beta} 0} \hat{R}_o \hat{R}_p + 3\chi_{iik}^{\alpha 0 \bar{\alpha} 0} \bar{\mu}_l^{\beta 0 \bar{\beta} 0} \hat{R}_k \hat{R}_l \right. \\ - 9\chi_{iik}^{\alpha 0 \bar{\alpha} 0} \bar{\mu}_l^{\beta 0 \bar{\beta} 0} \hat{R}_k \hat{R}_l \hat{R}_o \hat{R}_p + 3\chi_{ijk}^{\alpha 0 \bar{\alpha} 0} \bar{\mu}_k^{\beta 0 \bar{\beta} 0} - 9\chi_{ijk}^{\alpha 0 \bar{\alpha} 0} \bar{\mu}_k^{\beta 0 \bar{\beta} 0} \hat{R}_o \hat{R}_p \\ - 9\chi_{ijk}^{\alpha 0 \bar{\alpha} 0} \bar{\mu}_l^{\beta 0 \bar{\beta} 0} \hat{R}_k \hat{R}_l + 27\chi_{ijk}^{\alpha 0 \bar{\alpha} 0} \bar{\mu}_l^{\beta 0 \bar{\beta} 0} \hat{R}_k \hat{R}_l \hat{R}_o \hat{R}_p - \chi_{iik}^{\beta 0 \bar{\alpha} 0} \bar{\mu}_k^{\alpha 0 \bar{\beta} 0} \\ + 3\chi_{iik}^{\beta 0 \bar{\alpha} 0} \bar{\mu}_k^{\alpha 0 \bar{\beta} 0} \hat{R}_o \hat{R}_p + 3\chi_{iik}^{\beta 0 \bar{\alpha} 0} \bar{\mu}_l^{\alpha 0 \bar{\beta} 0} \hat{R}_k \hat{R}_l - 9\chi_{iik}^{\beta 0 \bar{\alpha} 0} \bar{\mu}_l^{\alpha 0 \bar{\beta} 0} \hat{R}_k \hat{R}_l \hat{R}_o \hat{R}_p \\ + 3\chi_{ijk}^{\beta 0 \bar{\alpha} 0} \bar{\mu}_k^{\alpha 0 \bar{\beta} 0} - 9\chi_{ijk}^{\beta 0 \bar{\alpha} 0} \bar{\mu}_k^{\alpha 0 \bar{\beta} 0} \hat{R}_o \hat{R}_p - 9\chi_{ijk}^{\beta 0 \bar{\alpha} 0} \bar{\mu}_l^{\alpha 0 \bar{\beta} 0} \hat{R}_k \hat{R}_l \\ \left. + 27\chi_{ijk}^{\beta 0 \bar{\alpha} 0} \bar{\mu}_l^{\alpha 0 \bar{\beta} 0} \hat{R}_k \hat{R}_l \hat{R}_o \hat{R}_p \right] + \{\alpha \leftrightarrow \beta\}. \quad (3.20)$$

The differential rate therefore has a linear dependence on R in the near zone.

Systems involving two centers with fixed mutual orientation have been shown to exhibit other circular differential effects with a similar linear dependence on the separation. Examples include Rayleigh and Raman scattering^{7,8} and two-photon circular dichroism in which only one chromophore is excited.⁹

IV. TWO RANDOMLY ORIENTED MOLECULES

We now consider the case in which the two molecules involved in the interaction are free to take up any separation and any mutual orientation. In the last section both the molecular tensors of centers A and B and the R vector were referred to a system frame a fixed to center A, which was rotationally averaged with respect to the p frame containing the laser polarization vectors: The result was Eq. (3.3). Two further averages are required to derive a rate expression for the fluid phase. The first step involves specifying a molecule-fixed Cartesian reference frame b in which the molecular tensors of molecule B are rotationally invariant, and performing a rotational average with respect to the a frame. This step accounts for the rotation of molecule B relative to molecule A. The second step is carried out by specifying an r frame in which the R vectors are rotationally invariant, and subsequently averaging with respect to the a frame; this step accounts for the random orientation of the vector \mathbf{AB} relative to the molecule A.

Table I. Averaging scheme: p , a , b , and r are reference frames defined in the text.

Vector and tensor quantities	e	$(\chi^{\alpha 0}, \mu^{\alpha 0})$	$(\chi^{\beta 0}, \mu^{\beta 0})$	V	Result
Before averaging Eq. (2.13)	p	p	p	p	...
	\downarrow	\uparrow	\uparrow	\downarrow	
Rotational average $a \leftrightarrow p$	p	a	a	a	van der Waals rate Eq. (3.3)
	\downarrow	\downarrow	\downarrow	\downarrow	
Rotational average $b \leftrightarrow a$	p	a	b	a	...
	\downarrow	\downarrow	\downarrow	\downarrow	
Rotational average $r \leftrightarrow a$	p	a	b	r	Unpaired fluid rate Eq. (4.1)

The full averaging procedure is outlined in Table I, and the result after full averaging is

$$\Gamma = \frac{K}{12\,096\,000\pi^2 R^6} [\{ a(\chi_{ik}^{\alpha 0} \bar{\chi}_{jik}^{\alpha 0} \mu_i^{\beta 0} \bar{\mu}_i^{\beta 0}) + b(\chi_{ijk}^{\alpha 0} \bar{\chi}_{ijk}^{\alpha 0} \mu_i^{\beta 0} \bar{\mu}_i^{\beta 0}) + c(\chi_{ijk}^{\beta 0} \bar{\chi}_{ijl}^{\alpha 0} \mu_k^{\beta 0} \bar{\mu}_l^{\alpha 0}) + d(\chi_{kik}^{\beta 0} \bar{\chi}_{jil}^{\alpha 0} \mu_i^{\beta 0} \bar{\mu}_i^{\alpha 0}) + e(\chi_{iil}^{\beta 0} \bar{\chi}_{mij}^{\alpha 0} \mu_k^{\beta 0} \bar{\mu}_i^{\alpha 0}) + f(\chi_{kik}^{\beta 0} \bar{\chi}_{ijl}^{\alpha 0} \mu_i^{\beta 0} \bar{\mu}_i^{\alpha 0}) \} + \{ \alpha, p \leftrightarrow \beta, q \}] , \quad (4.1)$$

where

$$a = 5600(2\eta - 1)[3F(p,R)F(p,R) + 2F(p,R)G(p,R) + G(p,R)G(p,R)] , \quad (4.2)$$

$$b = 5600(3 - \eta)[3F(p,R)F(p,R) + 2F(p,R)G(p,R) + G(p,R)G(p,R)] , \quad (4.3)$$

$$c = 56j_0(2kR)[(2\eta - 1)\{300F(q,R)F(p,R) + 100F(q,R)G(p,R) + 100F(p,R)G(q,R) + 100G(p,R)G(q,R)\} + (3 - \eta)\{120F(q,R)F(p,R) + 40F(q,R)G(p,R) + 40F(p,R)G(q,R) + 36G(q,R)G(p,R)\}] - 20j_2(2kR)[(5\eta - 4)\{80F(q,R)G(p,R) + 80F(p,R)G(q,R) + 80G(q,R)G(p,R)\} + (3 - 2\eta)\{88F(q,R)G(p,R) + 88F(p,R)G(q,R) + 96G(q,R)G(p,R)\}] + 3j_4(2kR)(2 + \eta)[2600F(q,R)F(p,R) + 440F(q,R)G(p,R) + 440F(p,R)G(q,R) + 392G(q,R)G(p,R)] , \quad (4.4)$$

$$d = -56j_0(2kR)(3 - \eta)[60F(q,R)F(p,R) + 20F(q,R)G(p,R) + 20F(p,R)G(q,R) + 8G(q,R)G(p,R)] + 20j_2(2kR)[(5\eta - 4)\{120F(q,R)G(p,R) + 120F(p,R)G(q,R) + 120G(q,R)G(p,R)\}] + (3 - 2\eta)\{104F(q,R)G(p,R) + 104F(p,R)G(q,R) + 128G(q,R)G(p,R)\}] + 3j_4(2kR)(2 + \eta)[-800F(q,R)F(p,R) + 480F(q,R)G(p,R) + 480F(p,R)G(q,R) + 624G(q,R)G(p,R)] , \quad (4.5)$$

$$e = -56j_0(2kR)(3 - \eta)[60F(p,R)F(q,R) + 20F(q,R)G(p,R) + 20F(p,R)G(q,R) + 8G(q,R)G(p,R)] + 20j_2(2kR)[(5\eta - 4)\{60F(q,R)F(p,R) + 120F(q,R)G(p,R) + 120F(p,R)G(q,R) + 120G(q,R)G(p,R)\}] + (3 - 2\eta)\{104F(q,R)G(p,R) + 104F(p,R)G(q,R) + 128G(q,R)G(p,R)\}] + 3j_4(2kR)(2 + \eta)[-800F(q,R)F(p,R) + 80F(q,R)G(p,R) + 80F(p,R)G(q,R) + 224G(q,R)G(p,R)] , \quad (4.6)$$

$$f = 56j_0(2kR)(3 - \eta)[180F(q,R)F(p,R) + 60F(q,R)G(p,R) + 60F(p,R)G(q,R) + 24G(q,R)G(p,R)] + 20j_2(2kR)(3 - 2\eta)[168F(q,R)G(p,R) + 168F(p,R)G(q,R) + 96G(q,R)G(p,R)] + 3j_4(2kR)(2 + \eta)[2400F(q,R)F(p,R) + 1360F(q,R)G(p,R) + 1360F(p,R)G(q,R) + 928G(q,R)G(p,R)] . \quad (4.7)$$

Despite the complexity of this result it is immediately apparent that there are no j_1 or j_3 terms and hence, as we would expect, circular dichroism is not exhibited in this case within the electric dipole approximation. Note also that the only dependence on the laser polarization is through η , in the coefficients a to f , defined by Eq. (3.4).

The overall R dependence of the rate is determined by the R^{-6} term in Eq. (4.1), by the spherical Bessel functions in Eqs. (4.2) to (4.7), and also by $F[p(q),R]$ and $G[p(q),R]$. Two limits can be considered. The expression for the cooperative absorption rate in the near zone where $(2k,p,q) \ll R^{-1}$ may be derived from Eq. (4.1) using the limiting results given in Eqs. (3.15), (3.16), and (3.17), with the result being a simple R^{-6} dependence. In the far zone where $(2k,p,q) \gg R^{-1}$, the limiting behaviors of $F(p,R)$ and $G(p,R)$ are given by

$$\lim_{pR \gg 1} F(p,R) = -p^2 R^2 \cos^2 pR , \quad (4.8)$$

$$\lim_{pR \gg 1} G(p,R) = p^2 R^2 \cos^2 pR , \quad (4.9)$$

and it can be shown that all of the spherical Bessel functions j_n for $0 \leq n \leq 4$, average to zero for large values of R . As a result, the only terms retained in Eq. (4.1) are the first two, with coefficients a and b , and the rate therefore has an R^{-2} dependence. Both the limiting near-zone and far-zone dependence on R are the same as for the alternative cooperative two-photon absorption mechanism discussed previously.¹

V. DISCUSSION

The work in this paper complements that of our first paper on cooperative two-photon absorption, in which we dealt with the 2,2-allowed mechanism, appropriate to the case of transitions forbidden under single-photon selection rules. The theoretical methods used are the same in both cases, and lead to general results applicable to either electronic or vibrational transitions in interacting pairs of molecules.

Important differences arise from the selection rules involved in the process. In the 3,1-mechanism described in this paper, both molecular excited states are reached through either a one- or a three-photon process, and in the general case, both one- and three-photon transitions are allowed at each center; hence the rate Eqs. (3.3) and (4.1) have terms with the transposition ($\alpha \leftrightarrow \beta$). However, if for example the selection rules in molecule B do not allow three-photon transitions $|\beta\rangle \leftarrow |0\rangle$, then these terms are not included in the rate

expressions. This corresponds to the omission of the 12 time-ordered diagrams of the type shown in Figs. 1(c) and 1(d) from the summation for M_{β} in Eq. (2.5). This situation does not arise in the 2,2-allowed mode in which all 24 diagrams always contribute.

Before proceeding further with our discussion, we should note that it is perfectly possible for both the 2,2-allowed and the 3,1-allowed mechanisms to occur, if the molecules A and B both lack inversion symmetry. In such a case, the rate of cooperative two-photon absorption includes not only the results given in papers I and II, but also additional terms resulting from the interference of probability amplitudes associated with the two mechanisms. However, these terms contain no new physics, and lead to R dependence of the same form as already described. We shall therefore concentrate on the more interesting case in which two-photon transitions $|\alpha\rangle\leftarrow|0\rangle$ and $|\beta\rangle\leftarrow|0\rangle$ are forbidden in the separate molecules A and B, and the 3,1-mechanism provides the only route for cooperative two-photon excitation to take place. Let us first consider a feature which distinguishes this mechanism from that discussed in paper I.

One of the principal differences between the 2,2- and 3,1-mechanisms lies in the range over which the limiting near-zone behavior occurs. In the 2,2 case, the near zone is defined by $\gamma R \ll 1$, where $\hbar\gamma = \frac{1}{2}(E_{\beta 0} - E_{\alpha 0})$ represents half the difference in the excited state energies of A and B. However, in the 3,1- case, the most severe constraints for the near-zone behavior are imposed by the conditions $pR \ll 1$ and $qR \ll 1$, where $\hbar q = E_{\alpha 0}$ and $\hbar p = E_{\beta 0}$ represent the actual excited state energies of A and B. In certain cases significant differences in the range of the near-zone result from this distinction.

Extreme differences are observed when the excited state energies are large but similar. In paper I we considered the specific example of cooperative $2_0^1 4_0^3$ transitions in the mixture of formaldehyde and deuterioformaldehyde, associated with wave numbers 30 340.15 and 30 147.62 cm^{-1} , respectively. In the 2,2-mode, the near-zone R^{-6} dependence of the rate extends to values of R up to $\sim 10^4$ nm. However in the 1,3-mode, the near-zone behavior should only extend to ~ 100 nm, and the far-zone R^{-2} behavior should be dominant at $R \approx 10^4$ nm.

At the other extreme, we may consider a cooperative process in which one center undergoes an electronic or vibrational transition, and the other center a purely vibrational transition. In this case the 2,2-allowed mode exhibits near-zone behavior over a much reduced range of values of R ; the 1,3-mode shows a new effect. The assumption that the wave vectors p and q are of similar magnitude, and of the same order as k , is no longer valid in this situation: if the electronic transition is at A, e.g., we have the condition that $q \gg p$. When we consider the near and far zone we thus find that, for certain values of R the functions $F(p, R)$ and $G(p, R)$ will show the near-zone behavior of Eq. (3.14), whereas $F(q, R)$ and $G(q, R)$ will show the far-zone behavior of Eq. (4.10), leading to an overall R^{-4} rate dependence.

It is possible to estimate the magnitude of the cooperative two-photon process by assuming typical values for the transition dipole moments and energies in the χ_{ijk}^{fo} tensor.

For intermolecular distances R comparable to molecular dimensions the rate is of the same order as one-center two-photon absorption, diminishing with increasing separation by a factor of R^{-6} in the near zone. However, it is important to consider the precise structure of the molecular transition tensor as defined by Eq. (2.6).

Clearly resonance enhancement of the rate may be expected if any of the energy denominators in the tensor approaches zero. There are four different terms in these denominators, and the resonance conditions for each are discussed below, assuming that the three-photon transition takes place at center A.

(a) Resonance behavior is expected if an intermediate state $|s\rangle$ exists with energy $\approx E_0 + 2\hbar\omega$. In this case, however, competition from simple two-photon absorption $|s\rangle\leftarrow|0\rangle$ must occur, and the cooperative effect will most likely be swamped.

(b) Similarly, the single-photon resonance associated with the state $|r\rangle$ where $E_r \approx E_0 + \hbar\omega$ will be dominated by single-photon absorption.

(c) A third resonance is expected for a state $|r\rangle$ of energy $E_\alpha + 2\hbar\omega$, but it is clear from the energy level diagram [Fig. 2(a)] that this condition cannot be satisfied if the cooperative transition takes place from the ground state. These three resonance conditions therefore cannot lead to any useful enhancement of the process.

(d) The fourth resonance is important however, and corresponds to the case where we have a state $|s\rangle$ of energy $E_s \approx E_\alpha - \hbar\omega$; in this case there is no possibility of competition from single-photon or two-photon absorption, but the cooperative absorption rate should be significantly increased.

We have assumed for this last case that $E_\alpha > E_\beta$ as illustrated in Fig. 2(a); if however $E_\beta > E_\alpha$ as in Fig. 2(b) then this resonance also disappears. In summary if the three-photon interaction takes place at center A, then resonance enhancement of the rate will occur only if $E_\alpha > E_\beta$ and an intermediate state $|s\rangle$ exists satisfying $E_\alpha - \hbar\omega \approx E_s$. Precisely analogous arguments apply if the three-photon transition occurs at B, reversing the roles of α and β in the above discussion.

We have noted that the tensor χ_{ijk}^{fo} is identical to the hyper-Raman scattering tensor. The order of enhancement factor for this tensor on resonance under typical conditions has been considered by Long and Stanton¹⁰ who give a typical value of as much as 10^6 . Clearly such a large increase will be a significant consideration in an experimental study of the effect.

Finally, it is interesting to note that the 3,1-mechanism requires only the molecule undergoing the three-photon transition to be in the laser beam, the one-photon transition resulting from virtual photon coupling. While this is not expected to lead to any significant enhancement of the rate, the effect could be directly observable if the single-photon excited state were fluorescent. The focused laser beam should then be surrounded by a halo of light of a different frequency. Observation of such an effect would clearly show that 1,3-allowed two-photon-cooperative absorption was taking place. It may also be possible to directly observe the decrease in fluorescent intensity according to the R^{-2} law predicted

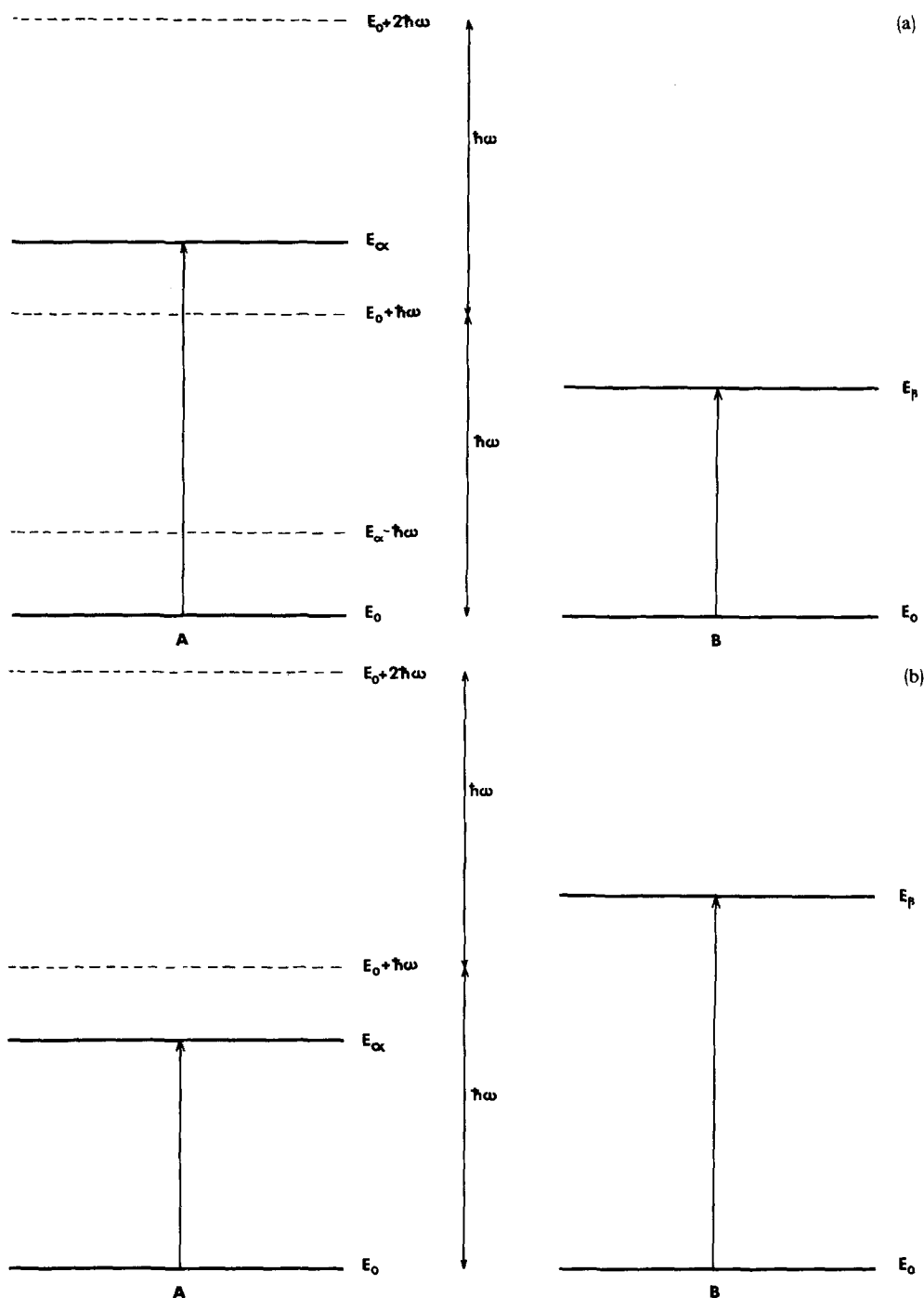


FIG. 2. Energy level diagrams.

for the far zone, although intensities would be extremely low.

CORRECTION

In paper I we note that in Eq. (2.2) we should have d^{12} not d^{13} .

ACKNOWLEDGMENT

M. J. H. gratefully acknowledges financial support from the Science and Engineering Research Council.

¹D. L. Andrews and M. J. Harlow, *J. Chem. Phys.* **78**, 1088 (1983).

²D. L. Andrews and T. Thirunamachandran, *J. Chem. Phys.* **68**, 2941 (1978).

³E. A. Power, *Introductory Quantum Electrodynamics* (Longmans, New York, 1964).

⁴E. Fermi, *Nuclear Physics* (University of Chicago, Chicago, 1950).

⁵D. L. Andrews and T. Thirunamachandran, *J. Chem. Phys.* **67**, 5026 (1977).

⁶D. L. Andrews and M. J. Harlow, *Phys. Rev. A* (to be published).

⁷L. D. Barron and A. D. Buckingham, *J. Am. Chem. Soc.* **96**, 4769 (1974).

⁸D. L. Andrews and T. Thirunamachandran, *Proc. R. Soc. London Ser. A* **358**, 297 and 311 (1978).

⁹D. L. Andrews, *Chem. Phys.* **16**, 419 (1976).

¹⁰D. A. Long and L. Stanton, *Proc. R. Soc. London Ser. A* **318**, 441 (1970).